



Published in final edited form as:

J Cereb Blood Flow Metab. 2007 ; 28: 431–438.

Early Beneficial Effect of Matrix Metalloproteinase Inhibition on BBB Permeability as Measured by MRI Countered by Impaired Long-Term Recovery After Stroke in Rat Brain

Rohit Sood, MD, PhD^{1,4}, Saeid Taheri, PhD^{1,4}, Eduardo Candelario-Jalil, PhD¹, Eduardo Y. Estrada, BS¹, and Gary A. Rosenberg, MD^{1,2,3}

¹Department of Neurology, Health Sciences Center, UNM

²Department of Neuroscience, Health Sciences Center, UNM

³Department of Cell Biology and Physiology, Health Sciences Center, UNM

⁴The BRaIN center, UNM

Abstract

Proteolytic disruption of the extracellular matrix with opening of the blood-brain barrier (BBB) due to MMPs occurs in reperfusion injury after stroke. MMP inhibition blocks the early disruption of the BBB, but the long-term consequences of short-term MMP inhibition are not known. Recently, a method to quantify BBB permeability by graphical methods was described that provides a way to study both early disruption of the BBB and long-term effects on recovery in the same animal. We used a broad-spectrum MMP inhibitor, BB1101, to determine both the usefulness of the MRI method for treatment studies and the long-term effects on recovery. MRI studies were performed in control (N=6) and drug treated (N=8) groups on a dedicated 4.7T MRI scanner. Adult WKY rats had a 2 hr MCAO and an MRI study after 3 hrs of reperfusion, which consisted of T2 and diffusion-weighted technique. Additionally, a rapid T1 mapping protocol was also implemented to acquire one pre-Gd-DTPA baseline data set followed by post injection data sets at 3 min intervals for 45 min. The same animal was imaged again at 48 hrs for lesion size estimation. Data was post processed pixel-wise to generate ADC and permeability coefficient maps. Treatment with BB-1101 significantly reduced BBB permeability at 3 hrs, but failed to reduce lesion size at 48 hrs. Behavioral studies showed impairment in recovery in treated rats. MRI allowed for the monitoring of multiple parameters in the same animal. Our studies showed that BB-1101 was an excellent inhibitor of the BBB damage. However, results show that BB-1101 may be responsible for significant deterioration in neurological status of treated animals. While these preliminary results suggest that BB-1101 is useful in reducing early BBB leakage due to reperfusion injury in stroke, further studies will be needed to determine whether the later detrimental effects can be eliminated by shorter time course of drug delivery.

Keywords

MRI; BB1101; T1; permeability; BBB; lesion size

Introduction

Matrix metalloproteinases (MMPs) are expressed in ischemic brain tissue as part of a molecular cascade that is initiated by the loss of blood supply by thrombus or an embolus (Mun-Bryce

and Rosenberg 1998b). Thrombolysis with recombinant tissue plasminogen activator (rtPA) restores the flow of oxygenated blood to the ischemic region. However, treatment with rtPA needs to be started within three hours of stroke onset because reperfusion causes a transient opening of the blood brain barrier (BBB), allowing rtPA and other substances in the blood to enter the brain (Tsirka 1997), (Wang et al. 1998). It has been shown that disruption of the blood-brain barrier (BBB), which occurs early after the onset of reperfusion, results in the extravasation of rtPA into the brain, where it increases the risk of bleeding (Kelly et al. 2006). BBB disruption is mediated by the action of MMP at the neurovascular unit (Rosenberg et al. 1998), initiated in part by intrinsic expression and activation of matrix metalloproteinase (MMPs) by central nervous system (CNS) astrocytes and microglia in response to hypoxia/ ischemia.

MMPs, a subfamily of metalloproteinases, are traditionally recognized as matrix degrading enzymes involved in tissue remodeling during development and homeostasis and have been implicated in normal and pathological functions within nervous system including stroke (Yong et al. 2001). MMP-2 is constitutively expressed by astrocytes, MMP-9 is secreted mainly by blood vessels, neurons and inflammatory cells and MMP-3 is mainly secreted by neurons, microglia and pericytes. Numerous studies suggest that opening of the BBB in focal cerebral ischemia results from activation and expression of MMPs. Following the early transient BBB opening, there is a second phase of severe BBB injury causing hemorrhagic transformation that is associated with marked elevation of MMP-9 expression.

Recently, we have shown that a constitutive MMP, gelatinase A (MMP-2), which is activated by membrane-type metalloproteinase (MT-MMP) early after the onset of reperfusion, disrupts the tight junction proteins (Yang et al. 2007), allowing substances such as rtPA, in the circulation, into the brain. There is increasing evidence that synthetic inhibitors to MMPs are able to prevent the disruption of the endothelial cells, preserving the integrity of the BBB, preventing the extravasation of rtPA and extending the therapeutic window for the use of thrombolytics. MMPs have beneficial actions, in addition to the detrimental ones that are found in the early stages of reperfusion; they are important in the recovery phase where they facilitate angiogenesis (Lee et al. 2006) and neurogenesis (Wang et al. 2006a). Therefore, it is important to be able to test both the short-term beneficial actions and the long-term detrimental actions of the MMP inhibitors in order to identify agents that could be used therapeutically.

MRI offers the means to measure BBB permeability and infarct size without sacrificing the animal so that long term behavioral studies can be performed. An MRI based method to estimate the blood-to-brain transfer constant, k_i (or barrier permeability coefficient) using standardized techniques has been described (Ewing et al. 2003). The MRI technique for estimating barrier permeability coefficient, k_i , is based on a graphical analysis method (Blasberg et al. 1983). This technique involves quantifying distribution of gadolinium-diethylenetriaminepentaacetic acid (Gd-DTPA), an MRI contrast agent, in the brain tissue. Recently, we have used the MRI-based graphical analysis method for testing the BBB blocking properties of propylene glycol (Sood et al. 2007). Therefore, the non-invasive MRI method for quantifying BBB permeability appears to be an appropriate technique for investigating the effect of BB-1101, a broad spectrum MMP inhibitor, on BBB disruption.

Several laboratories have demonstrated in different models that broad-spectrum MMP inhibitor, BB-94 (Batimastat), blocked the BBB damage, but they did not study the long-term effects of the drug (Paul et al. 1998), (Pfefferkorn and Rosenberg 2003). It is possible that the therapeutic window for the use of MMP inhibitors could be narrow, and that understanding the long-term consequences of the use of these agents will be critical. We have used the MRI based multiple time graphical analysis method to study the effect of a synthetic MMP inhibitor, BB-1101, on early BBB permeability. Additionally, MRI has been used to make measurements

of stroke infarct size at 48 hrs and behavior over 4 weeks. In this way, the full impact of the drug in multiple stages of injury and recovery was investigated effectively.

Thus, the aims of this study were 1) to investigate the BBB blocking property of BB-1101 using MRI at 3 hrs post middle cerebral artery occlusion (MCAO) in a rat ischemic stroke model; 2) to investigate the effect of BB-1101 on lesion size at 48 hrs post MCAO using MRI; 3) to evaluate the effect of BB-1101 on neurological function by performing behavioral studies in treated and control rats.

Materials and Methods

MCAO

The study was approved by the Local Animal Research Committee and conformed to the National Institutes of Health guidelines for use of animals in research. Wistar-Kyoto (WKY) rats weighing 250 – 300 gm underwent 2 hrs of MCAO followed by reperfusion for 3 hrs. Rats were anesthetized with 2% isoflurane during the surgery. The MCAO technique has been described previously (Sood et al. 2007). Briefly, neck vessels were exposed through a midline incision. After isolation and ligation of the branches of the right external carotid vessels, a 6–0 silk suture was loosely tied around the external carotid artery stump. A section of 4–0 monofilament nylon suture was introduced into the external carotid artery and advanced to occlude the origin of the middle cerebral artery. The suture around the stump was tied down onto the nylon suture with the end of the suture protruding slightly. The middle cerebral artery was occluded for two hours. The thread was slowly pulled back to the external carotid stump for 3 hours of reperfusion.

MRI technique

MR imaging study was performed in a rat brain MCAO model of ischemic stroke. Animals were anesthetized using isoflurane gas (induction dosage 2–3%; maintenance dosage 1.5–2%) and a mixture of O₂:N₂O gases in the ratio 2:1 were delivered during the entire duration of the study. Real time monitoring of physiological parameters (heart rate and respiratory rate) was performed during the entire duration of the study. A PE-50 polyethylene catheter was placed into the femoral vein of each animal for injection of Gd-DTPA during the entire duration of the study.

In this study, 23 male Wistar Kyoto (WKY) rats in the weight range 250–300g were divided into two groups: the first group consisting of 12 rats that had MCAO but were not treated with the drug and served as controls, while the second group consisting of 11 rats, were treated with BB-1101. The treated animals were injected intraperitoneally (i.p.) with 30 mg/kg of BB-1101 diluted in 1ml of 0.9% saline. The drug was injected at T=0 (before MCAO) and at T=24 hrs and T=48 hrs post MCAO. The experimental design is shown in Figure 1. Rats were imaged at 3 hrs post MCAO for estimation of BBB permeability and then at 48 hrs post MCAO for estimation of ischemic lesion size. Each rat underwent behavioral study weekly for duration of 4 weeks. Out of the 11 rats treated with BB-1101, data from 6 rats was used for permeability analysis. This was due to technical reasons related to animals; two rats did not have visible evidence of ischemic lesion (determined on diffusion weighted MRI) probably due to failed surgery and three had evidence of intracerebral hemorrhage. Data from 4 control rats was excluded due to technical reasons related to MRI problems; evidence of artifacts on MR images due to magnetic shimming issues and/or gradient instability resulted in inability to perform analysis. Infarct size estimation was performed in 5 BB-1101 treated rats since in the treated group two rats (in addition to those not used for permeability analysis) did not survive till the 48hrs time point.

Rats were then transported to the MRI room, placed in a dedicated rat holder and moved to the isocenter of the magnet prior to the imaging session. MR imaging was performed on a 4.7T Biospec® dedicated research MR scanner (Bruker Biospin, Billerica, MA).

The MRI study was implemented in two sessions. In the first session, animals were brought to the MRI suite for imaging at 4.5 hrs post MCAO. At this stage, data was acquired for quantifying BBB permeability. The details of the scan parameters used in this MRI protocol are described below. Initial localizer images were acquired using the following parameters:

2D FLASH (Fast Low Angle SHot), TR/TE 10/3 ms, matrix 256×128 , FOV 6.4 cm, 1 slice per orientation. After the localizer images were acquired, T2 weighted and diffusion weighted imaging (DWI) was performed using parameters described in (Sood et al. 2007). The MR protocol for acquiring data for the Patlak plot method was then implemented. In this acquisition, a reference baseline acquisition using the fast T1 mapping protocol was obtained prior to injecting the contrast agent. 0.1mM/kg of Gd-DTPA (Berlex Lab, Montville, NJ) (Molecular weight 938 Da) was injected as a bolus into the femoral vein via the indwelling catheter, followed by imaging with rapid T1 mapping protocol for a total time of 45 minutes, resulting in a total of 14 time points. Gd-DTPA is about twice the molecular weight of [^{14}C]sucrose (342 Da), while it is small in comparison to [^{14}C]dextran (molecular weight 50–90 kDa) (Mun-Bryce and Rosenberg 1998a).

At 48 hrs, the rats were brought back for imaging of lesion size. MRI was performed using the following parameters: Initial localizer images were acquired using parameters as described earlier. After the localizer images were acquired, T2 weighted and DWI was performed with the following parameters; T2 weighted-2D turbo RARE (Rapid Acquisition with Relaxation Enhancement), TR/TE 4000/65 ms, matrix 256×128 , number of averages 22, echo train length 8; DWI - 2D Diffusion weighted RARE, TR/TE 2000/31.2 ms, matrix 64×64 , number of averages 15, $d = 5$ ms, $D = 20$ ms, b value of 0 and 927 s mm^{-2} , diffusion gradient along the slice select direction. Common acquisition parameters were FOV $3.2 \text{ cm} \times 3.2 \text{ cm}$, slice thickness 2 mm, slice gap 0 mm, number of slices 14, receiver bandwidth 100 kHz. The slice prescriptions for T2 and diffusion weighted acquisitions were matched for all slice locations.

The acquired data from two MRI sessions was transferred to a dedicated computer workstation for post processing, image analysis and archiving. Post processing of the raw data involved generating Apparent Diffusion Coefficient (ADC) maps from DWI images, T1 maps from the raw data, reconstruction of permeability coefficient maps, construction of the Patlak plots and lesion volume estimation.

All the data processing was performed using in-house software written in 64bit MATLAB (Mathworks, MA) and implemented on a 64bit processor (AMD64) workstation running Red Hat Enterprise Linux v3 (64bit). Image analysis was performed using ImageJ (NIH, Bethesda) and MRVision (Winchester, MA) software.

Image analysis was performed using the methods described previously (Sood et al. 2007). Prior to analysis of permeability coefficient maps, Kalman filtering was performed on raw and processed data at two stages, first, on the series of inversion recovery echo images (12 frames per time point per slice) and second, on T1 maps over the entire time series, using a technique described previously (Taheri and Sood 2006). The permeability maps were also used for estimating area of leakage i.e. region of BBB disruption. The area of leakage was calculated as a product of number of pixels with high permeability and pixel size.

Lesion size estimation was performed on ADC maps reconstructed from multi slice DW images acquired at 48hrs using MRVision software 1.67 (MRVision, Winchester, MA). The multi slice diffusion weighted acquisition was prescribed such that whole rat brain coverage was

obtained. All the acquired slices were used for lesion size analysis. ADC maps were reconstructed pixel-wise from diffusion weighted data such that pixel signal intensity values were proportional to absolute ADC values. Lesion size was measured using various ADC thresholds, and was defined as area with ADC values < 80% of the mean contralateral hemisphere values on the ADC map (Hoehn-Berlage et al. 1995) (Figure 2). The analysis was performed by a single operator and the procedure was repeated twice. Lesion size, reported by the software, was calculated as number of pixels \times pixel size, where the number of pixels, were pixels with values less than the ADC threshold value. Lesion size was estimated per slice and reported as sum over the total number of prescribed slices. These estimates were saved as a text file, read into Excel spreadsheet (Microsoft, Redmond) and used for further analysis.

Behavior studies

The effect of BB-1101 on neurological function was evaluated using behavioral studies. Behavioral assessments were made every week post surgery for 4 weeks by evaluating the animals using tests that measure neurological deficit. Briefly, the rats were tested and scored for neurological deficits as follows, 0 - No apparent deficit; 1 - Failure to extend left forepaw; 2 - Decreased grip of the left forelimb while tail is pulled or twisting entire body toward contralateral side; 3 - Spontaneous movement in all directions, circling to left only if pulled by tail, or falling to the contralateral side and 4 - Spontaneous circling to the left or no spontaneous walking with reduced level of consciousness or inability to walk spontaneously and 5 - death of the animal. Each test was graded as 1 if positive and 0 if negative.

Statistical analysis

Permeability coefficient data obtained from MRI experiments was analyzed using a one-way ANOVA (Analysis of Variance) statistical test. Permeability coefficient values obtained from ROI analysis of the ipsilateral and contralateral side and infarct lesion sizes from control and treated groups were read into Microsoft excel software (Microsoft, Redmond) for statistical data analysis. The results obtained from ANOVA statistical analysis for the MRI technique was presented as Mean \pm standard error of mean (S.E.M).

Results

Figure 3 shows a series of T2 weighted images, DW contrast images and color-coded permeability coefficient maps for two representative rats; treated (top row) and control (bottom row). The T2 weighted images demonstrated the lesion in relation to the anatomical detail in the rat brain.

In the control group, ADC values in the rat brain were estimated to be $0.46 \pm 0.19 \times 10^{-3} \text{ mm}^2 \text{ s}^{-1}$ (mean \pm SD) and $0.95 \pm 0.21 \times 10^{-3} \text{ mm}^2 \text{ s}^{-1}$ on the ipsilateral and contralateral hemisphere respectively. ADC values estimated in treated rats on the ipsilateral and contralateral side were $0.42 \pm 0.06 \times 10^{-3} \text{ mm}^2 \text{ s}^{-1}$ and $0.79 \pm 0.04 \times 10^{-3} \text{ mm}^2 \text{ s}^{-1}$ respectively. The ADC value in the ipsilateral ROI dropped 48.4% of the matching contralateral areas in control group and 53.1% in BB-1101 treated rats respectively, after 3 hrs of reperfusion.

Figure 4 shows a graph of mean permeability coefficient values in control group and treated group estimated using MRI. There was a significant ($p < 0.05$) reduction observed in mean permeability coefficient values on the ipsilateral side in the drug treated rats as compared to the untreated rats.

The area of leakage estimated from enhancing pixels on the permeability map in control and drug treated rats was $7.70 \pm 1.70 \text{ mm}^2$ and $1.24 \pm 0.78 \text{ mm}^2$ respectively. There was a

statistically significant ($p < 0.05$) difference in the area of leakage between control and treated groups.

Figure 5 shows a plot of individual lesion size measured at 48 hrs in control and treated rats. The stroke lesion size in the control and treated group was $213.4 \pm 49.3 \text{ mm}^2$ and $223.7 \pm 69.6 \text{ mm}^2$ respectively. There was no significant difference in lesions size between the control and treated groups.

Behavioral study results shown in Figure 6 show that there was a statistically significant increase in neurological deficit in the 3rd and 4th week in rats treated with BB-1101 as compared to control ($p < 0.05$).

Discussion

Reperfusion of ischemic tissue causes enhanced production of free radicals (Chan et al. 1984), release of proteases (Gidday et al. 2005), and a biphasic opening of the BBB (Kuroiwa et al. 1985). The hemorrhagic conversion occurs in approximately 60% of patients after an embolic stroke (Hornig et al. 1993). Use of rtPA carries the risk of increasing the incidence of symptomatic hemorrhage ten times. Leakage of rtPA across a damaged BBB is potentially toxic to the brain cells (Kaur et al. 2004). There is sufficient evidence to support the fact that activation of MMPs by rtPA plays a significant role in causing hemorrhage and that synthetic MMP inhibitors prevent the BBB opening and protect the brain from rtPA toxicity. In this work, we have investigated the ability of an hydroxymate MMP inhibitor, BB-1101, to block BBB leakage and its effect on stroke lesion size using MRI. The multiple graphical analysis method implemented using MRI, is based on the model of unidirectional tracer kinetics in one compartment and provides a noninvasive approach to investigate the BBB blocking properties of novel pharmaceutical agents without sacrificing the animal. This in turn enables subsequent estimation of stroke lesion size at 48hrs post MCAO and evaluation of neurological function.

The permeability coefficient maps were reconstructed from Kalman filtered data. Digital Kalman filtering (Kalman 1960) is a robust adaptive filtering technique that optimally estimates, in real time, the state of a system (true MR signal) based on its noisy outputs. The technical details of the filtering technique and its application to improving the reliability of permeability coefficient estimates is described elsewhere (Taheri and Sood 2006). As a result, application of this filtering technique, allowed reliable estimation of permeability maps from data that has low signal to noise ratio (SNR), a drawback of fast MR data acquisition techniques such as IR-SE-EPI. In the treated group, the permeability coefficient values on the ischemic side ($0.77 \pm 0.31 \times 10^{-3} \text{ ml g}^{-1} \text{ min}^{-1}$) and the non-ischemic side ($0.31 \pm 0.21 \times 10^{-3} \text{ ml g}^{-1} \text{ min}^{-1}$) were well within the range for permeability coefficient values in healthy tissue ($0 - 1 \times 10^{-3} \text{ ml g}^{-1} \text{ min}^{-1}$), suggesting that BB-1101 was successful in reducing BBB permeability on the ischemic side. On comparing permeability coefficient values for ipsilateral side, a 75% reduction in mean permeability coefficient values has been observed in treated group compared to the control group. The reduction in permeability coefficient values due to BB-1101 treatment was found to be statistically significant ($p < 0.05$). The MRI provided both a permeability coefficient and a spatial map of the permeability changes. This suggests that BB-1101 may be working to reduce BBB leakage in the region of maximal ischemic injury and confirms both the utility of the Patlak plot graphical method for measuring drug effects and the earlier findings by us (Rosenberg et al. 1998), using an invasive BBB permeability measurement technique, that BB-1101 is effective in blocking the BBB leakage.

The lesion size at 48hrs was not significantly different between the treated and control groups. The lack of effect of BB-1101 on lesion size at 48hrs is consistent with earlier study showing that BB-1101 did not affect permeability at 48 hrs (Rosenberg et al. 1998). Interestingly, when

an MMP-9-neutralizing monoclonal antibody was administered systemically (Romanic et al. 1998), animals exhibited significantly reduced infarct size (a 30% reduction was observed compared with non-immune antibody controls; $p < 0.05$). However, this difference between the antibody and the synthetic inhibitor is difficult to explain and warrants further investigation.

ADC maps obtained from whole rat brain were used for performing lesion size estimation since they provide a reliable way of measuring damaged tissue due to ischemia compared to signal intensity based methods. In this study, ischemic tissue was defined as region with ADC values less than 80% of the normal values. Published research suggests that using 80% ADC threshold at early MR imaging has the strongest correlation with histopathological analysis and is the only independent significant variable affecting irreversible infarct volume (Wang et al. 2006b). Additionally, ADC threshold set at approximately 80% of the normal ADC has been found to correlate well with the loss of ATP and breakdown of energy metabolism in animal studies of focal cerebral ischemia both during ischemia and reperfusion (Olah et al. 2000). At 3 hrs post MCAO, BB-1101 did not have effect on the ADC values in the treated groups suggesting that the drug may not have a neuroprotective effect. Regional cerebral blood flow (rCBF) studies were not done in this work and may have potentially provided helpful insight into the neuroprotective effect of BB-1101. In this study, the absolute ADC values obtained in this study for healthy rat brain tissue are higher than those found in the literature (ADC values for healthy rat brain tissue are in the range $0.6 - 0.7 \times 10^{-3} \text{ mm}^2 \text{ s}^{-1}$) (Does and Gore 2000). One possible explanation for this finding would be motion induced artifact during data acquisition.

Behavior study results in the treated group showed a significant increase in neurological deficit at 3 and 4 week period, suggesting the detrimental effects of BB-1101 on neurological function. In the control group, the deficit appeared to decrease over the 4 weeks period of evaluation. The lack of long-term benefit from a broad spectrum inhibitor was seen in a recent study that showed the inhibition of MMP blocks angiogenesis and neurogenesis, which interfered with recovery (Zhao et al. 2006). We removed one high permeability coefficient value in a BB-1101 treated animal because it was an extreme outlier. The high permeability value was observed due to the leakage of Gd-DTPA into the cerebrospinal fluid space resulting in very high and inaccurate permeability estimates.

In conclusion, BB-1101, an MMP inhibitor, appears to be a promising candidate for BBB blockage during the early phase of BBB disruption. The drug did not have any effect on stroke lesion size at 48hrs post MCAO and had significant adverse effects on neurological function in rats at 3 and 4 weeks post MCAO. Future studies will need to define the optimal timing of delivery of a MMP inhibitor so that the BBB damage is blocked and that there is no interference with recovery.

Acknowledgements

Grant support: NIH grant RO1NS045847 to GAR. NIH COBRE grant 5P20RR15636-05 to RS and ST.

References

- Blasberg RG, Fenstermacher JD, Patlak CS. Transport of alpha-aminoisobutyric acid across brain capillary and cellular membranes. *J Cereb Blood Flow Metab* 1983;3:8–32. [PubMed: 6822623]
- Chan PH, Schmidley JW, Fishman RA, Longar SM. Brain injury, edema, and vascular permeability changes induced by oxygen-derived free radicals. *Neurology* 1984;34:315–320. [PubMed: 6546610]
- Does MD, Gore JC. Compartmental study of diffusion and relaxation measured in vivo in normal and ischemic rat brain and trigeminal nerve. *Magn Reson Med* 2000;43:837–844. [PubMed: 10861878]

- Ewing JR, Knight RA, Nagaraja TN, Yee JS, Nagesh V, Whitton PA, Li L, Fenstermacher JD. Patlak plots of Gd-DTPA MRI data yield blood-brain transfer constants concordant with those of ¹⁴C-sucrose in areas of blood-brain opening. *Magn Reson Med* 2003;50:283–292. [PubMed: 12876704]
- Gidday JM, Gasche YG, Copin JC, Shah AR, Perez RS, Shapiro SD, Chan PH, Park TS. Leukocyte-derived matrix metalloproteinase-9 mediates blood-brain barrier breakdown and is proinflammatory after transient focal cerebral ischemia. *Am J Physiol Heart Circ Physiol* 2005;289:H558–568. [PubMed: 15764676]
- Hoehn-Berlage M, Norris DG, Kohno K, Mies G, Leibfritz D, Hossmann KA. Evolution of regional changes in apparent diffusion coefficient during focal ischemia of rat brain: the relationship of quantitative diffusion NMR imaging to reduction in cerebral blood flow and metabolic disturbances. *J Cereb Blood Flow Metab* 1995;15:1002–1011. [PubMed: 7593332]
- Hornig CR, Bauer T, Simon C, Trittmacher S, Dorndorf W. Hemorrhagic transformation in cardioembolic cerebral infarction. *Stroke* 1993;24:465–468. [PubMed: 8446984]
- Kalman RE. A new approach to linear filtering and prediction problems. *Transactions of ASME-Journal of Basic Engn* 1960;82:35–45.
- Kaur J, Zhao Z, Klein GM, Lo EH, Buchan AM. The neurotoxicity of tissue plasminogen activator? *J Cereb Blood Flow Metab* 2004;24:945–963. [PubMed: 15356416]
- Kelly MA, Shuaib A, Todd KG. Matrix metalloproteinase activation and blood-brain barrier breakdown following thrombolysis. *Exp Neurol* 2006;200:38–49. [PubMed: 16624294]
- Kuroiwa T, Ting P, Martinez H, Klatzo I. The biphasic opening of the blood-brain barrier to proteins following temporary middle cerebral artery occlusion. *Acta Neuropathol (Berl)* 1985;68:122–129. [PubMed: 3907257]
- Lee SR, Kim HY, Rogowska J, Zhao BQ, Bhide P, Parent JM, Lo EH. Involvement of matrix metalloproteinase in neuroblast cell migration from the subventricular zone after stroke. *J Neurosci* 2006;26:3491–3495. [PubMed: 16571756]
- Mun-Bryce S, Rosenberg GA. Gelatinase B modulates selective opening of the blood-brain barrier during inflammation. *Am J Physiol* 1998a;274:R1203–1211. [PubMed: 9644031]
- Mun-Bryce S, Rosenberg GA. Matrix metalloproteinases in cerebrovascular disease. *J Cereb Blood Flow Metab* 1998b;18:1163–1172. [PubMed: 9809504]
- Olah L, Wecker S, Hoehn M. Secondary deterioration of apparent diffusion coefficient after 1-hour transient focal cerebral ischemia in rats. *J Cereb Blood Flow Metab* 2000;20:1474–1482. [PubMed: 11043910]
- Paul R, Lorenzl S, Koedel U, Sporer B, Vogel U, Frosch M, Pfister HW. Matrix metalloproteinases contribute to the blood-brain barrier disruption during bacterial meningitis. *Ann Neurol* 1998;44:592–600. [PubMed: 9778257]
- Pfefferkorn T, Rosenberg GA. Closure of the blood-brain barrier by matrix metalloproteinase inhibition reduces rtPA-mediated mortality in cerebral ischemia with delayed reperfusion. *Stroke* 2003;34:2025–2030. [PubMed: 12855824]
- Romanic AM, White RF, Arleth AJ, Ohlstein EH, Barone FC. Matrix metalloproteinase expression increases after cerebral focal ischemia in rats: inhibition of matrix metalloproteinase-9 reduces infarct size. *Stroke* 1998;29:1020–1030. [PubMed: 9596253]
- Rosenberg GA, Estrada EY, Dencoff JE. Matrix metalloproteinases and TIMPs are associated with blood-brain barrier opening after reperfusion in rat brain. *Stroke* 1998;29:2189–2195. [PubMed: 9756602]
- Sood R, Taheri S, Estrada EY, Rosenberg GA. Quantitative evaluation of the effect of propylene glycol on BBB permeability. *J Magn Reson Imaging* 2007;25:39–47. [PubMed: 17173307]
- Taheri S, Sood R. Kalman filtering for reliable estimation of BBB permeability. *Magn Reson Imaging* 2006;24:1039–1049. [PubMed: 16997074]
- Tsirka SE. Clinical implications of the involvement of tPA in neuronal cell death. *J Mol Med* 1997;75:341–347. [PubMed: 9181475]
- Wang L, Zhang ZG, Zhang RL, Gregg SR, Hozeska-Solgot A, LeTourneau Y, Wang Y, Chopp M. Matrix metalloproteinase 2 (MMP2) and MMP9 secreted by erythropoietin-activated endothelial cells promote neural progenitor cell migration. *J Neurosci* 2006a;26:5996–6003. [PubMed: 16738242]

- Wang Y, Cheung PT, Shen GX, Wu EX, Cao G, Bart I, Wong WH, Khong PL. Hypoxic-ischemic brain injury in the neonatal rat model: relationship between lesion size at early MR imaging and irreversible infarction. *AJNR Am J Neuroradiol* 2006b;27:51–54. [PubMed: 16418355]
- Wang YF, Tsirka SE, Strickland S, Stieg PE, Soriano SG, Lipton SA. Tissue plasminogen activator (tPA) increases neuronal damage after focal cerebral ischemia in wild-type and tPA-deficient mice. *Nat Med* 1998;4:228–231. [PubMed: 9461198]
- Yang Y, Estrada EY, Thompson JF, Liu W, Rosenberg GA. Matrix metalloproteinase-mediated disruption of tight junction proteins in cerebral vessels is reversed by synthetic matrix metalloproteinase inhibitor in focal ischemia in rat. *J Cereb Blood Flow Metab* 2007;27:697–709. [PubMed: 16850029]
- Yong VW, Power C, Forsyth P, Edwards DR. Metalloproteinases in biology and pathology of the nervous system. *Nat Rev Neurosci* 2001;2:502–511. [PubMed: 11433375]
- Zhao BQ, Wang S, Kim HY, Storrie H, Rosen BR, Mooney DJ, Wang X, Lo EH. Role of matrix metalloproteinases in delayed cortical responses after stroke. *Nat Med* 2006;12:441–445. [PubMed: 16565723]

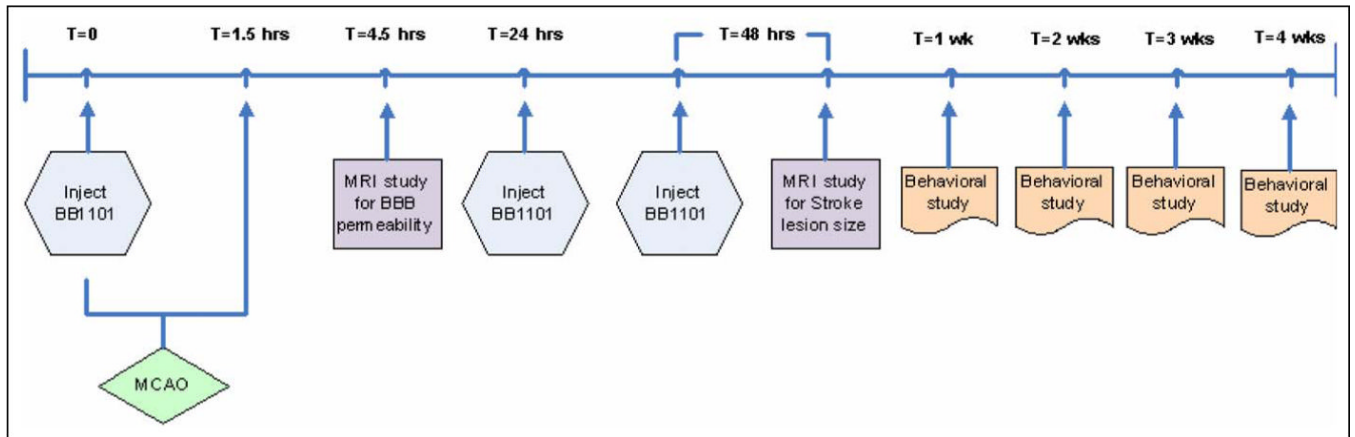


Figure 1. Flow chart providing an overview of the study. Please see text for more details on MCAO surgery, BB1101 injection dose, MRI protocol and behavior assessment.

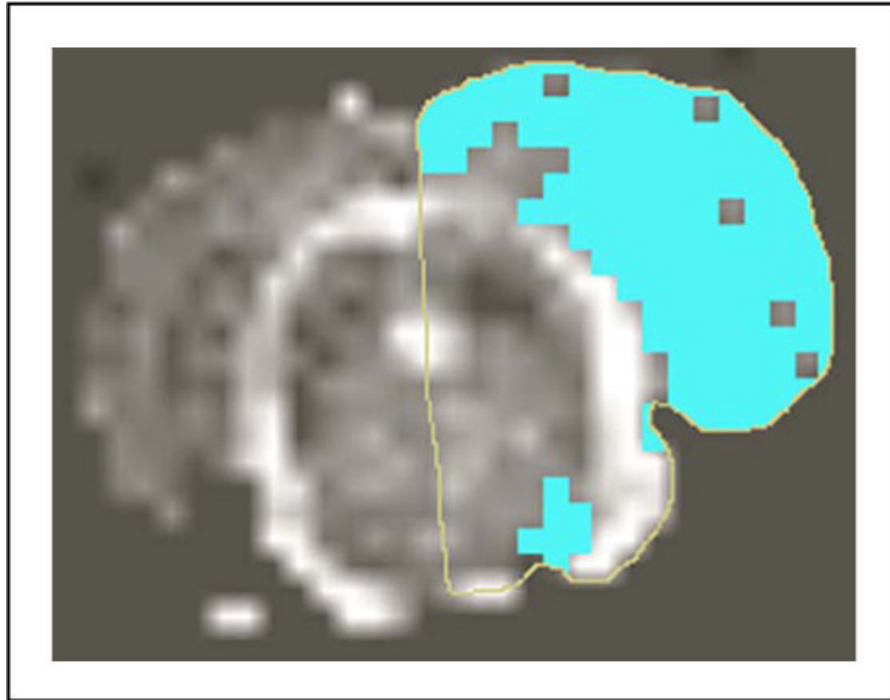


Figure 2. Shows lesion size estimation from ADC map using MRVision software. Thresholding technique was used to extract lesion pixels on the ipsilateral hemisphere with ADC values < 80% of the contralateral side.

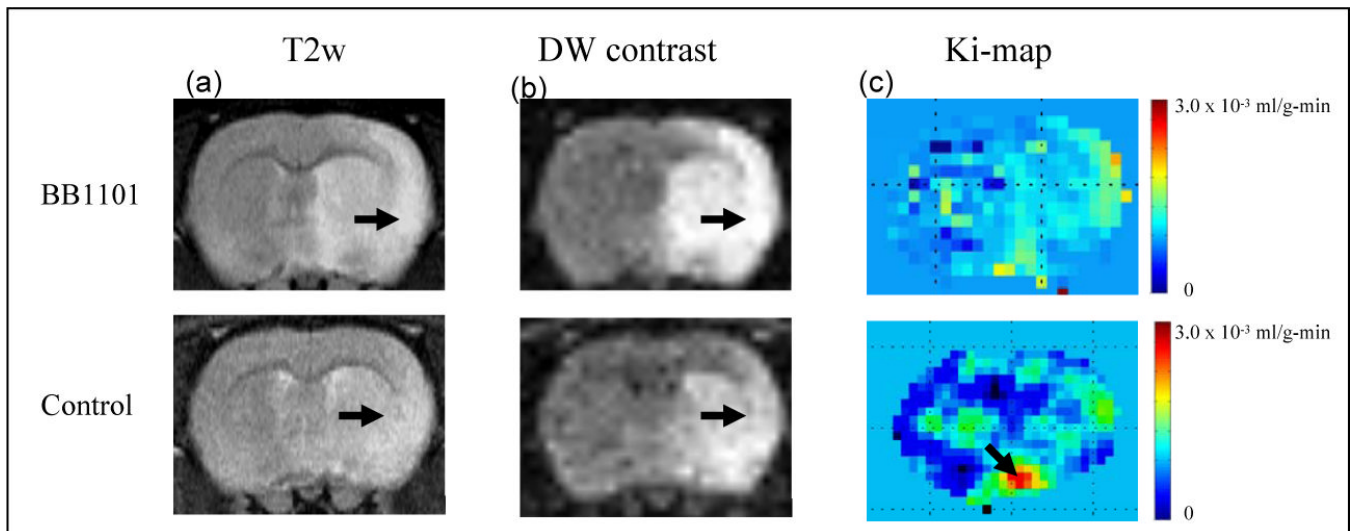


Figure 3. shows (a) T2 weighted image (b) DW contrast image (c) color coded permeability coefficient map for BB1101 treated (top row) and control (bottom row) rats. The ischemia can be seen as an hyperintense lesion (arrow) on T2 weighted images. A 53.1% and 48.4% reduction in the ADC value on the ischemic side (ROI on lesion) compared to that in the matching contralateral side was observed in BB1101 treated and control rats respectively, after 3 hours of reperfusion. The arrows on DW contrast image point at ischemic regions with diffusion changes. Color coded permeability maps demonstrate clearly the regions of high (arrow) and low permeability in treated and control rats.

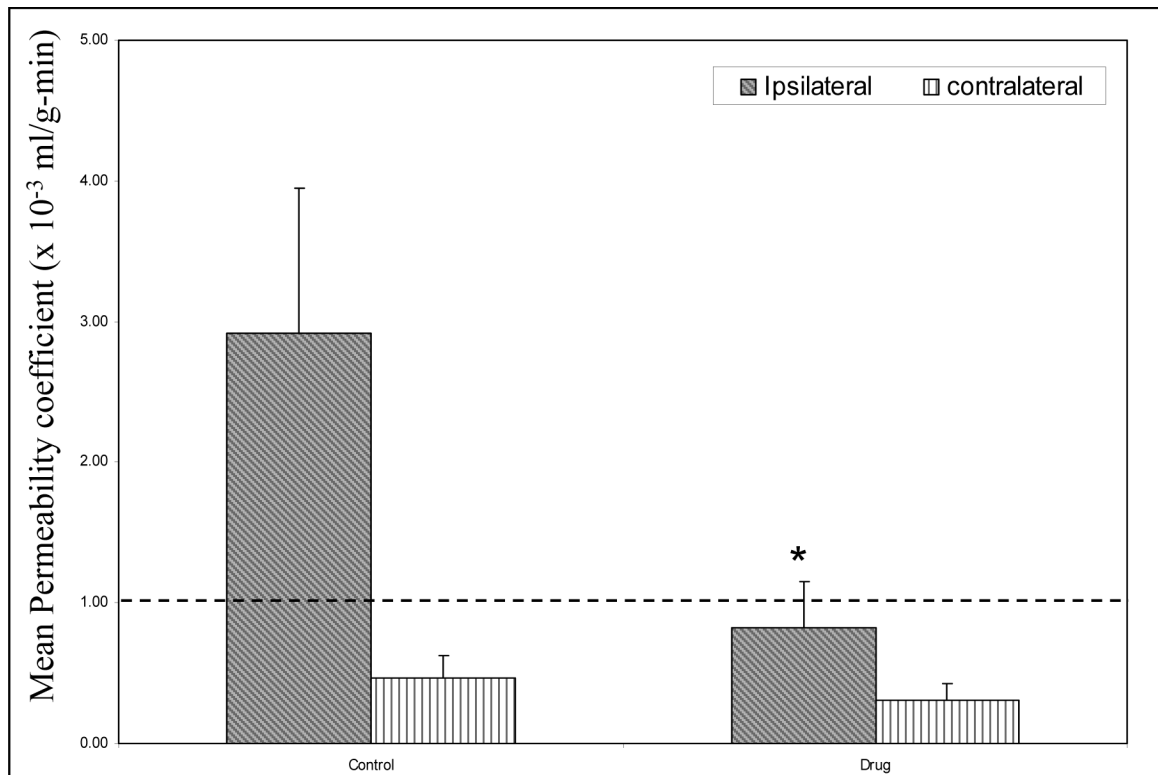


Figure 4.

A plot of mean permeability coefficient estimates in treated (N=6) and control (N=8) rats obtained using the MRI technique. The dashed line represents the upper limit of the range ($0 - 1 \times 10^{-3}$ ml/g-min) of permeability coefficient values in healthy tissue. Rats treated with BB1101 demonstrated a significant reduction in permeability coefficient values on the ischemic side as compared to the untreated rats (ANOVA, $*p < 0.05$, * indicates significant reduction). No significant difference was observed on the contralateral side between the control and treated rats. The Y axis error bars represent standard error of mean.

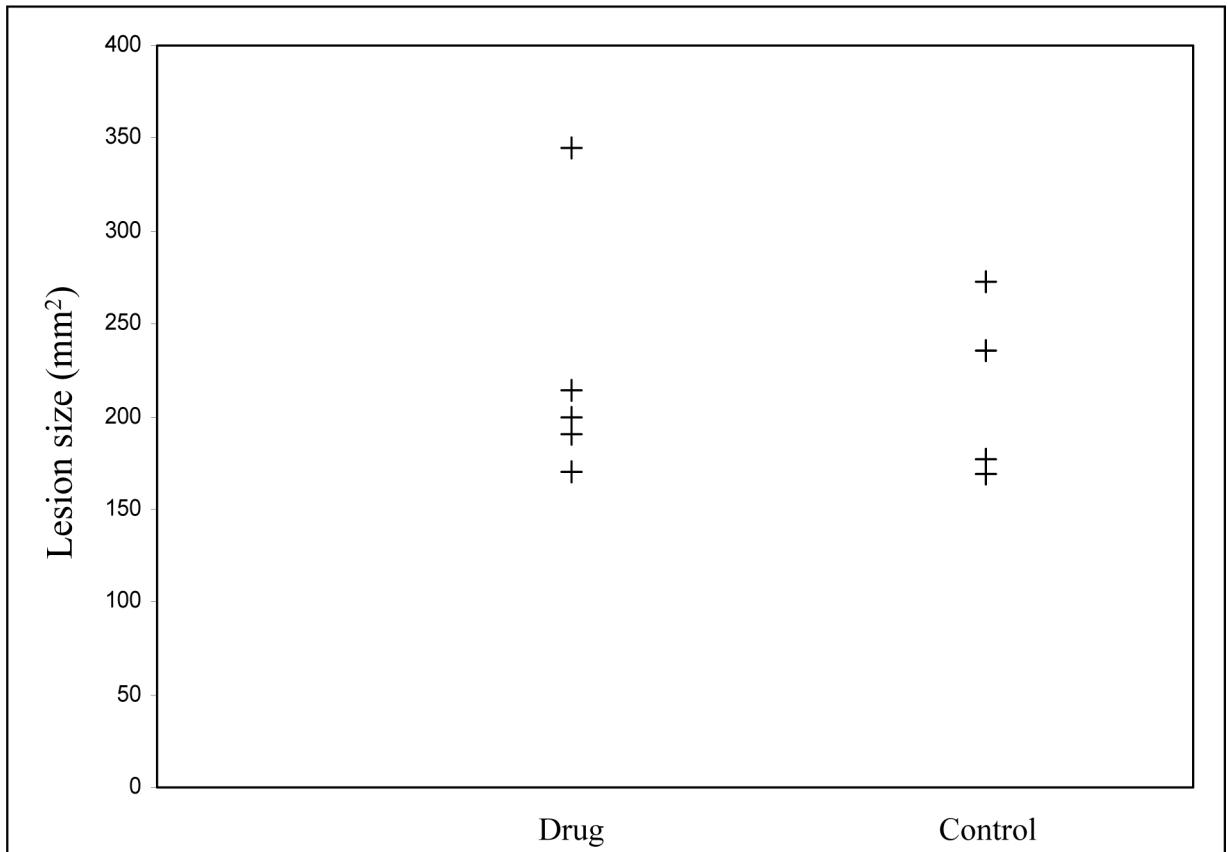


Figure 5.

Stroke lesion size in treated and control groups at 48 hrs after a 90-min MCAO. The lesion size in drug treated and control group was $223.7 \pm 69.6 \text{ mm}^2$ and $213.4 \pm 49.3 \text{ mm}^2$ respectively. There was no significant difference in lesion size observed between the two groups.

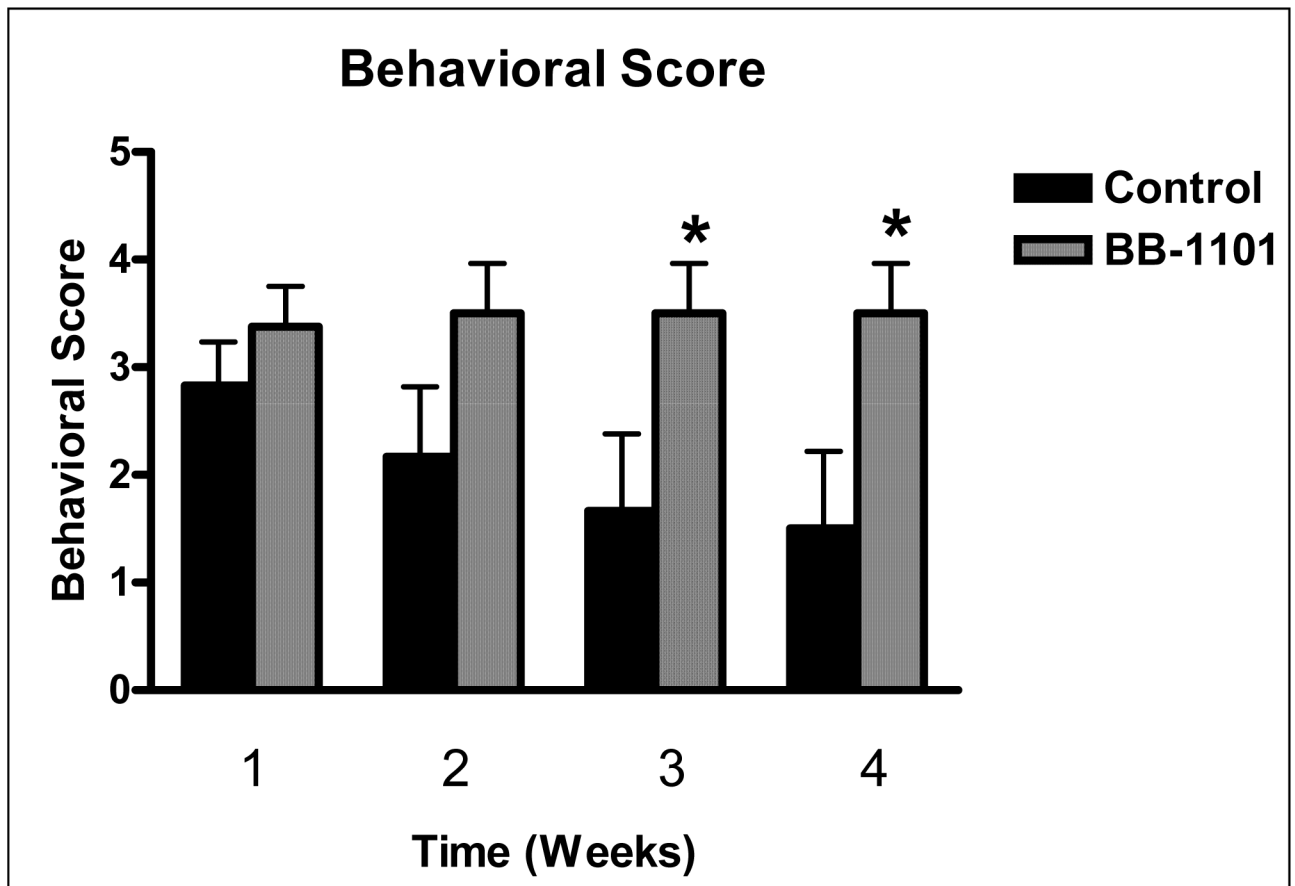


Figure 6. Behavioral scores in rats treated with BB-1101 and control group. Scoring was based on a 5 point scale and was done at weekly intervals for a duration of 4 weeks. There was a statistically significant increase in behavioral scores in the 3rd and 4th weeks. * $p < 0.05$.